Detection of Retinal Vessel Bifurcations by Means of Multiple Orientation Estimation Based on Regularized Morphological Openings

Álvar-Ginés Legaz-Aparicio[1], Rafael Verdú-Monedero[1], Juan Morales-Sánchez[1], Jorge Larrey-Ruiz[1], and Jesús Angulo[2]

[1] Universidad Politécnica de Cartagena, Dept. de Tecnologías de la Información y las Comunicaciones, Cartagena, Spain
[2] MINES Paristech, CMM-Centre de Morphologie Mathématique, Mathématiques et Systèmes, Fontainebleau Cedex, France

Abstract—**This paper describes an approach to detect vessel bifurcations and crossovers in retinal images. This approach is based on an novel method to estimate multiple orientations at each pixel of a gray image. The main orientations are provided by directional openings whose outputs are regularized in order to extend the orientation information to the whole image. The detection of vessel bifurcations is based on the coexistence of two or more than two different main orientations in the same pixel. Results on retinal images show the robustness and accuracy of the proposed method to detect vessel bifurcations.**

Keywords—**multiple orientation estimation, retinal fundus, vessel bifurcations.**

I. INTRODUCTION

The analysis of retinal vascular structures has a great use in medical analysis. Specifically, the identification and study of bifurcations and crossovers has great significance in cardiovascular diseases as well as in their early detection [1]. There are two approaches to detect automatically vessel bifurcations: methods based on geometrical features and methods based on models [2]. The method proposed in this paper belongs to the first group, it depends on the segmentation of the retinal image.

The segmentation of the vessel tree can be performed by matched filters [3], by region growing and scale-space analysis [4], by mathematical morphology [5], etc. Regarding the detection of vessel bifurcations and crossovers on segmented retinal images it can be done, e.g., by using a set of trainable keypoint detectors and a bank of Gabor filters [6], or with matched filters [7]. This paper addresses the detection of vessel bifurcations by analyzing a vectorial orientation field provided by the regularization of directional morphological openings.

The morphological orientation field [8] is given by a directional signature for each pixel using a series of directional openings with a line segment. Then, the orientation of a pixel is defined as the one associated to the directional opening which produces the maximal value of signature at the pixel. Nevertheless, the original approach from [8] does not deal with the multiple orientation case: locally, pixels in natural images can be associated to more than one orientation,

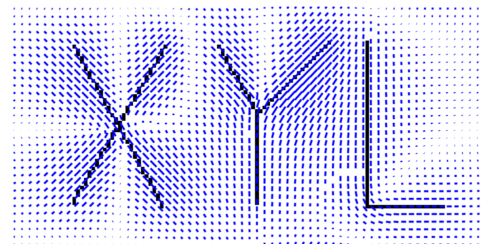

Fig. 1 Orientation vector field obtained by ASGVF [12] using η=1. The size of the image is 128× 64 pixels.

e.g., crossing lines, corners and junctions (also known as X-, L- and Y-junctions, respectively). To determine not only the main direction but all the significant orientations, the directional signature is analyzed in the present work using multiple peak detection on the curve interpolated by b-splines.

This paper is organized as follows: Section II-A addresses the method to estimate multiple orientations at each pixel and II-B describes the approach followed to detect the bifurcations and crossovers in retinal images. In Section III we apply the method in a retinal image, and finally, Section IV closes the paper with the conclusions and future work.

II. PROPOSED METHOD

In previous works of the authors, the orientation field was based on the average squared gradient (ASG) (see e.g. [10]). This orientation field is valid in images where only one main orientation exists at each pixel. When a pixel is close to edges with different orientations, the ASG provides an orientation which is a linear combination of these near orientations (as can be seen in Fig.1). The method proposed here to estimate multiple orientations is depicted in Fig. 2. This approach differs from [11], where the multiple main orientations are estimated by analyzing a block of the image, whereas in this paper the multiple orientations are estimated at each pixel.

A. Multiple Orientation Estimation

Let $f(\mathbf{x}) : E \to \mathbb{R}$ be a gray-level image, where the support space is $E \subset \mathbb{Z}^2$ and the pixel coordinates are $\mathbf{x} = (x, y)$. Let

L.M. Roa Romero (ed.), *XIII Mediterranean Conference on Medical and Biological Engineering and Computing 2013,*
IFMBE Proceedings 41,
DOI: 10.1007/978-3-319-00846-2_79,

us define $g(\mathbf{x})$ as the absolute value of the gradient of $f(\mathbf{x})$, i.e., $g(\mathbf{x}) = \|\nabla f(\mathbf{x})\|$.

The directional opening of $g(\mathbf{x})$ by a linear (symmetric) structuring element (SE) of length l and direction θ is defined as the directional erosion of g by $L^{\theta,l}$ followed by the directional dilation with the same SE [10]:

$$\gamma_{L^{\theta,l}}(g)(\mathbf{x}) = \delta_{L^{\theta,l}}\left[\varepsilon_{L^{\theta,l}}(g)\right](\mathbf{x}). \tag{1}$$

We remind that the subgraph of the opened image by $L^{\theta,l}$ is equivalent to the union of the translations of the linear SE when it fits the subgraph of the original image [13], or in other terms, bright linear image structures that cannot contain $L^{\theta,l}$ are removed by the opening.

The proposed orientation model is based on a decomposition of the gradient information by families of linear openings. Let $\{\gamma_{L^{\theta_i,l}}\}_{i\in I}$ be a family of linear openings of length l according to a particular discretization of the orientation space $\{\theta_i\}_{i\in I}$. In mathematical morphology theory, this parameterized family of openings is called a granulometry [13]. The granulometry is applied to the gradient image $g(\mathbf{x})$, i.e., for each orientation an opened image of the intensity gradient information is obtained. In addition, the accumulation by supremum of the openings (which has also the properties of an opening [13], i.e., idempotency and anti-extensivity) produces also an approximation of $g(\mathbf{x})$ at linear scale l, denoted $a_l^{\Theta}(g)(\mathbf{x})$:

$$a_l^{\Theta}(g)(\mathbf{x}) = \bigvee_{i\in I} \gamma_{L^{\theta_i,l}}(g)(\mathbf{x}). \tag{2}$$

The accumulation image $a_l^{\Theta}(g)(\mathbf{x})$ extracts the linear structures of $g(\mathbf{x})$ whose length is longer than l. Hence, the residue between $g(\mathbf{x})$ and $a_l^{\Theta}(g)(\mathbf{x})$,

$$r_l^{\Theta}(g)(\mathbf{x}) = g(\mathbf{x}) - a_l^{\Theta}(g)(\mathbf{x}), \tag{3}$$

yields the image structures of length shorter than l, and $r_l^{\Theta}(g)(\mathbf{x})$ might be used in a multiscale approach as the source image in the following stage with a smaller l (see Fig. 3).

When dealing with discrete images, it is important to remember the effects of discretization. As described in [12], the angular resolution of a structuring element of length l is $\Delta\theta = \frac{90}{l-1}$ degrees, therefore the angles that can be used are $\theta_i = i\Delta\theta$, $i \in I = [0, 2(l-1)-1]$. A long structuring element allows for a larger angular resolution (i.e., more directions) but the structures to be detected have to be bigger. On the other hand, a smaller structuring element offers fewer directions but it allows get into small details in the image.

In the next step of the proposed method a regularization is performed at each one of the directional openings (depicted as H_η in Fig. 2). The regularization diffuses the orientation information and avoid angle mismatches due to noise. Each

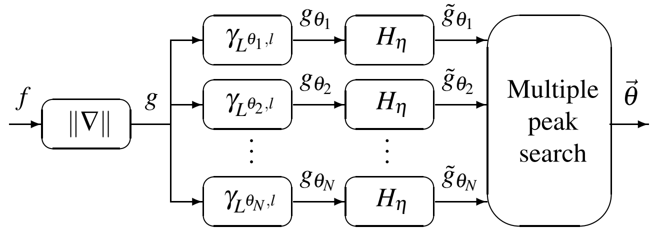

Fig. 2 Flowchart of the multiple orientation estimation method.

one of the regularized openings, $\tilde{g}_{\theta_i}$, minimizes the following energy functional

$$\mathscr{E}(\tilde{g}_{\theta_i}) = \mathscr{D}(\tilde{g}_{\theta_i}) + \alpha\mathscr{S}(\tilde{g}_{\theta_i}), \tag{4}$$

where $\mathscr{D}$ represents a distance measure given by the square difference between the original and the regularized directional opening, weighted by the squared value of the first one,

$$\mathscr{D}(\tilde{g}_{\theta_i}) = \frac{1}{2}\int_E ||g_{\theta_i}||^2 ||\tilde{g}_{\theta_i} - g_{\theta_i}||^2\, dx\, dy, \tag{5}$$

where E is the image support. The energy term $\mathscr{S}$ is the regularization term, it determines the smoothness of the regularized openings and represents the energy of the second order derivatives of the signal:

$$\mathscr{S}(\mathbf{v}) = \frac{1}{2}\int_E ||\Delta\tilde{g}_{\theta_i}||^2\, dx\, dy, \tag{6}$$

where $\Delta = \partial^2/\partial x^2 + \partial^2/\partial y^2$ is the Laplacian operator. The positive parameter α governs the trade off between the fit to g_{θ_i} and the smoothness of the solution $\tilde{g}_{\theta_i}$ (see e.g. [14]). According to the calculus of variations, the regularized opening $\tilde{g}_{\theta_i}$ minimizing Eq. (4) is necessarily a solution of the Euler–Lagrange equation:

$$(\tilde{g}_{\theta_i} - g_{\theta_i})|g_{\theta_i}|^2 + \alpha\Delta^2\tilde{g}_{\theta_i} = 0. \tag{7}$$

These equations can be solved by adding an artificial time and computing the steady-state solution. The solution is obtained by the following iterative implementation in the frequency domain

$$\tilde{G}^n_{\theta_i} = H_\eta(\tilde{G}^{n-1}_{\theta_i} + F^{n-1}) \tag{8}$$

where $\tilde{G}^n_{\theta_i}$ and $\tilde{G}^{n-1}_{\theta_i}$ are the 2D discrete Fourier transforms (DFT's) of their respective signals in the spatial domain, superscript n denotes the iteration index, F^{n-1} is the 2D DFT of $f^{n-1} = (g_{\theta_i} - \tilde{g}_{\theta_i})|g_{\theta_i}|^2$, H_η is the sampling of the low-pass filter

$$H_\eta(\omega_1, \omega_2) = \frac{\eta}{\eta + 4(2 - \cos\omega_1 - \cos\omega_2)^2}. \tag{9}$$

Once the directional openings have been regularized, the directional signature at pixel $\mathbf{x}$ is defined as

$$s_{\mathbf{x};l}(i) = \tilde{g}_{\theta_i}(\mathbf{x}). \tag{10}$$

$s_{\mathbf{x};l}(i)$ is interpolated using cubic b-splines and its detected maxima correspond to the multiple orientations existing at pixel $\mathbf{x}$. Collecting all the orientations estimated at all the pixels in the image provides the multidimensional vector field $\vec{\theta}(\mathbf{x})$ (see Fig. 6).

B. Detection of Bifurcations and Crossovers

Previous method can be applied on a gray image or on a binary image. However, most of the methods which detect bifurcations use a segmented, and therefore binary, image. In this paper we use a segmented image which contains the vessel tree to estimate the multiple orientation field, this orientation vector field is used then to detect the existing bifurcations and crossovers.

The detection procedure takes into account only the two main orientations at each pixel. The method considers that a bifurcation or crossover exists if two conditions happens. The first conditions is that the magnitude of the regularized opening has to be greater than a threshold, $|\tilde{g}_{\theta_i}| > th$. The second condition to be fulfilled is that two main orientations must differ more than $2\Delta\theta$ to avoid false positives due to high curvature of the vessels.

III. RESULTS

We have used a segmented retinal image from the DRIVE database [9] to evaluate the performance of the proposed method. Given that the size of this image is 565×584 pixels, the directional openings use an oriented linear structuring element of 7 pixels. This length comes from the tradeoff between the curvature of the vessels and the angular resolution of the structuring element (this length provides $\Delta\theta = 15°$ and produces a filter bank with 12 branches). The regularization of the directional openings is performed using η=1 and 10 iterations of the procedure given in eq. (8). Finally, the threshold th used to consider that a pixel belongs to a bifurcation or crossover is the 25% of the maximum intensity value.

As can be seen in Fig. 7, the proposed method detects all the bifurcations and crossovers, however, vessel with high curvature are also detected. In Fig. 8 a close-up of the retinal image with the multiple orientation vector field is shown.

(a) $g(\mathbf{x})$ (b) $a_l^{\Theta}(g)(\mathbf{x})$ (c) $r_l^{\Theta}(g)(\mathbf{x})$

Fig. 3 a) Absolute value of the gradient of $f(\mathbf{x})$, b) accumulation by supremum of directional openings, c) residue of the orientation apertures.

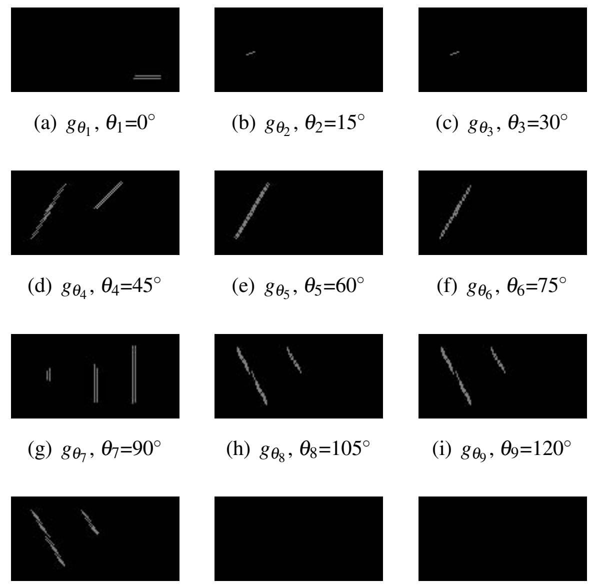

(a) g_{θ_1}, θ_1=0° (b) g_{θ_2}, θ_2=15° (c) g_{θ_3}, θ_3=30°
(d) g_{θ_4}, θ_4=45° (e) g_{θ_5}, θ_5=60° (f) g_{θ_6}, θ_6=75°
(g) g_{θ_7}, θ_7=90° (h) g_{θ_8}, θ_8=105° (i) g_{θ_9}, θ_9=120°
(j) $g_{\theta_{10}}$, θ_{10}=135° (k) $g_{\theta_{11}}$, θ_{11}=150° (l) $g_{\theta_{12}}$, θ_{12}=165°

Fig. 4 Directional openings of $g(\mathbf{x})$ with l=7.

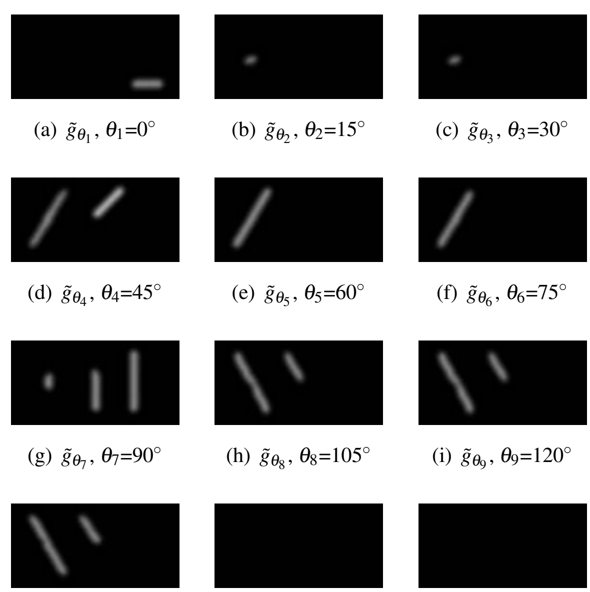

(a) $\tilde{g}_{\theta_1}$, θ_1=0° (b) $\tilde{g}_{\theta_2}$, θ_2=15° (c) $\tilde{g}_{\theta_3}$, θ_3=30°
(d) $\tilde{g}_{\theta_4}$, θ_4=45° (e) $\tilde{g}_{\theta_5}$, θ_5=60° (f) $\tilde{g}_{\theta_6}$, θ_6=75°
(g) $\tilde{g}_{\theta_7}$, θ_7=90° (h) $\tilde{g}_{\theta_8}$, θ_8=105° (i) $\tilde{g}_{\theta_9}$, θ_9=120°
(j) $\tilde{g}_{\theta_{10}}$, θ_{10}=135° (k) $\tilde{g}_{\theta_{11}}$, θ_{11}=150° (l) $\tilde{g}_{\theta_{12}}$, θ_{12}=165°

Fig. 5 Regularized directional openings using η=1.

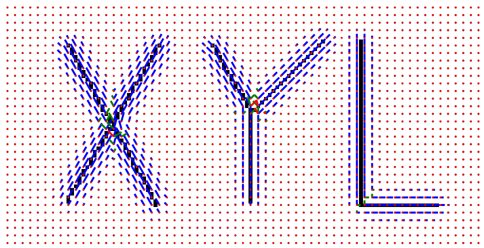

Fig. 6 Multiple orientation vector field $\vec{\theta}$ obtained by the proposed method.

IV. CONCLUSIONS

This paper has presented a method for the detection of bifurcations and crossovers based on a novel estimation of multiple orientations. The robustness of the morphological operators to provide the orientation vector field produces a correct detection of all bifurcations and crossovers, but also high curvature vessels are wrongly detected. Note that due to the regularization of the directional openings, resulting in an orientation discrimination, the proposed method is able to detect bifurcations with gaps which do not preserve completely the connectivity of the bifurcations.

As future work, we will evaluate the performance of the proposed method on all retinal images from DRIVE [9] and STARE [15] databases. Comparisons with other state-of-art methods as, e.g., [6], also will be done. Another task for further research and development is the analysis and post-processing of the results in order to detect vessels with high curvature and then try to reduce the false positives.

ACKNOWLEDGEMENTS

This work is supported by the Spanish Ministerio de Ciencia e Innovación, under grant TEC2009-12675.

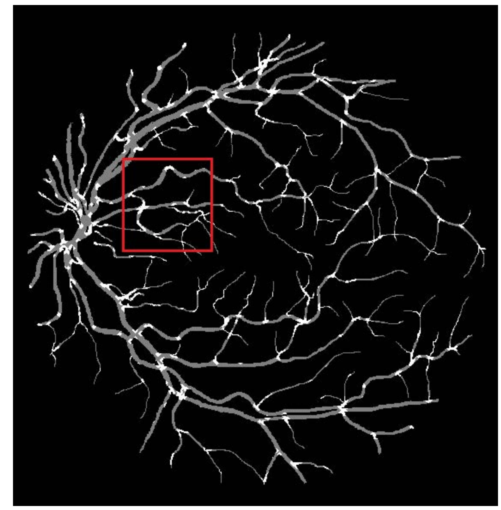

Fig. 7 Segmented retinal image *01_manual1* from DRIVE database [9] with detected bifurcations and crossovers.

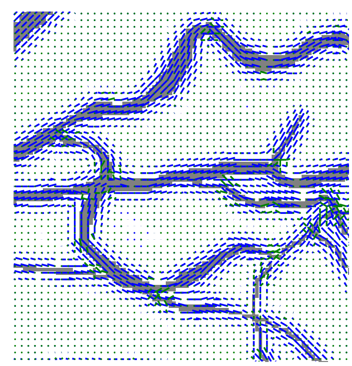

Fig. 8 Close up of the red square depicted on Fig. 7 with the multiple orientation vector field.

REFERENCES

1. Witt N., et al. Abnormalities of retinal microvascular structure and risk of mortality from ischemic heart disease and stroke *Hypertension.* 2006;47:975-981.
2. Abramoff M.D., Garvin M.K., Sonka M.. Retinal Imaging and Image Analysis *Biomedical Engineering, IEEE Reviews in.* 2010;3:169-208.
3. Chaudhuri S., Chatterjee S., Katz N., Nelson M., Goldbaum M.. Detection of blood vessels in retinal images using two-dimensional matched filters *IEEE Trans. Medical Imaging.* 1989;8:263-269.
4. Martínez-Pérez M. et al. Scale-space analysis for the characterisation of retinal blood vessels *MICCAI.* 1999:90-97.
5. Zana F., Klein J.-C.. Segmentation of vessel-like patterns using mathematical morphology and curvature evaluation *IEEE Trans. on Image Processing.* 2001;10:1010-1019.
6. Azzopardi G., Petkov N. Automatic detection of vascular bifurcations in segmented retinal images using trainable COSFIRE filters in *Pattern Recognition Letters*;34:922-933 2013.
7. Ardizzone E., Pirrone R., Gambino O., Radosta Salvatore. Blood vessels and feature points detection on retinal images *Engineering in Medicine and Biology Society.* 2008:2246-2249.
8. Soille P., Talbot H.. Directional Morphological Filtering *IEEE Trans. on Pattern Analysis and Machine Intelligence.* 2001;23:1313-1329.
9. Staal J. et al. Ridge-based vessel segmentation in color images of the retina *IEEE Trans Medical Imaging.* 2004;23:501-509.
10. Verdú-Monedero R., Angulo J., Serra J. Anisotropic Morphological Filters With Spatially-Variant Structuring Elements Based on Image-Dependent Gradient Fields *IEEE Trans. Image Processing.* 2011;20:200-212.
11. Angulo J., Verdú-Monedero R., Morales-Sánchez J. Multiscale local multiple orientation estimation using Mathematical Morphology and B-spline interpolation *ISPA.* 2011:575 - 578.
12. Verdú-Monedero R., Angulo J. Spatially-Variant Directional Mathematical Morphology Operators Based on a Diffused Average Squared Gradient Field *LNCS: ACIVS.* 2008;5259:542-553.
13. Soille Pierre. *Morphological Image Analysis*. Springer-Verlag 1999.
14. Engl H., Hanke Martin, Neubauer A.. *Regularization of Inverse Problems*;375 of *Mathematics and Its Applications*. Springer 2000.
15. Hoover A., Kouznetsova V., Goldbaum M.. Locating blood vessels in retinal images by piecewise threshold probing of a matched filter response *IEEE Trans on Medical Imaging.* 2000;19:203-210.